JPET Fast Forward. Published on September 6, 2005 as DOI: 10.1124/jpet.105.093427

JPET #93427

Pharmacological Characterization of Human and Murine Neuropeptide S Receptor Variants

Rainer K. Reinscheid, Yan-Ling Xu, Naoe Okamura, Joanne Zeng, Shinjae Chung, Rama Pai, Zhiwei Wang and Olivier Civelli

Department of Pharmacology (R.K.R., Y.L.X., N.O., J.Z., S.C., Z.W., O.C.), Department of Developmental and Cell Biology (O.C.), University of California Irvine, Irvine, California, 92697; Department of Gastroenterology (R.P.), Veterans Affairs Medical Center, Long Beach, California, 90822

JPET Fast Forward. Published on September 6, 2005 as DOI: 10.1124/jpet.105.093427
This article has not been copyedited and formatted. The final version may differ from this version.

a. Running Title: Pharmacology of NPS receptor variants

b. Address correspondence to: Rainer K. Reinscheid, Department of Pharmacology, University of California Irvine, 360 Med Surge II, Irvine, CA 92697-4625, Tel: 949 824-9228, Fax: 949 824-4855, E-Mail: rreinsch@uci.edu

c. Manuscript Information

Text Pages:		29
Tables:		1
Figures:		6
References:		13
Words in	Abstract:	231
	Introduction:	593
	Discussion:	1338

d. Nonstandard Abbreviations:

NPS, neuropeptide S; NPSR, neuropeptide S receptor; GPCR, G protein-coupled receptor; SNP, single nucleotide polymorphism; MAPK, mitogen-activated protein kinase;

e. Section Assignment: Cellular and Molecular

ABSTRACT

We have recently shown that Neuropeptide S (NPS) can promote arousal and induce anxiolytic-like effects after central administration in rodents. Another study reported a number of natural polymorphisms in the human NPS receptor gene. Some of these polymorphisms were associated with increased risk of asthma and possibly other forms of atopic diseases but the physiological consequences of the mutations remain unclear. One of the polymorphisms produces an Asn-Ile exchange in the first extracellular loop of the receptor protein and a C-terminal splice variant of the NPS receptor was found over-expressed in human asthmatic airway tissue. We sought to study the pharmacology of the human receptor variants in comparison with the murine receptor protein. Here we report that the Asn^{107}Ile polymorphism in the human NPS receptor results in a gain-of-function characterized by an increase in agonist potency without changing binding affinity in NPSR Ile^{107}. In contrast, the C-terminal splice variant of the human NPS receptor shows a pharmacological profile similar to NPSR Asn^{107}. The mouse NPS receptor, which also carries an Ile residue at position 107, displays an intermediate pharmacological profile. Structure-activity relationship studies show that the amino terminus of NPS is critical for receptor activation. The altered pharmacology of the Ile^{107} isoform of the human NPS receptor implies a mechanism of enhanced NPS signaling that might have physiological significance for brain function as well as peripheral tissues that express NPS receptors.

INTRODUCTION

Neuropeptide S (NPS) is the endogenous ligand of an orphan G protein-coupled receptor (GPCR). The NPS receptor (NPSR) belongs to the subfamily of peptide GPCRs and is widely expressed in the brain, with highest levels found in hypothalamus, amygdala, endopiriform nucleus, cortex, subiculum and nuclei of the thalamic midline. In contrast, the NPS precursor mRNA is found in only a few brain structures (Xu et al., 2004). Highest levels of NPS precursor expression were detected in a novel nucleus located in between the noradrenergic locus coeruleus (LC) and Barrington's nucleus in the pontine area of the rat brain stem. Other brain regions of high NPS precursor expression include the lateral parabrachial nucleus, sensory principle 5 nucleus and a few scattered neurons in the amygdala and dorsomedial hypothalamic nucleus. In addition, we found high expression of NPS and NPSR mRNA in endocrine tissues including thyroid, mammary and salivary glands but did not observe significant levels in rat lung tissue.

Central administration of NPS promotes behavioral arousal and suppresses all stages of sleep in rodents. Furthermore, NPS was found to produce anxiolytic-like effects in a battery of four different tests that measure behavioral responses of rodents to novelty or stress. NPS was shown to induce transient increases of intracellular Ca^{2+}, indicating that it might have excitatory effects at the cellular level (Xu et al., 2004).

Recently, a number of polymorphisms in the human NPS receptor gene were identified and a specific set of these polymorphisms was linked to an increased susceptibility for asthma and potentially other forms of allergy that are characterized by high IgE serum levels in Finnish and Canadian asthma patients (Laitinen et al., 2004). The study described a number of risk haplotypes and originally termed the receptor "GPRA isoform A" (for G protein-coupled receptor associated with asthma, GenBank accession no. NP_997055; the protein has also been termed GPR 154). This receptor protein is identical to the NPS receptor that we have studied extensively for its pharmacology, distribution and function in brain (Xu et al., 2004). One of the single-nucleotide polymorphisms changes the primary structure of the NPS receptor protein to code for an Asn-Ile exchange at position 107 of the mature protein (SNP591694 A>T; refSNP ID: rs324981; Fig. 1). The study also found that a C-terminal splice variant of the receptor, originally termed "GPRA isoform B" (GenBank accession no. NP_997056; Fig. 1), was over-expressed in human asthmatic airway tissue and that the orthologous murine receptor mRNA was upregulated in a mouse model of chronic airway inflammation. Immunostaining showed that human bronchial smooth muscle cells express the receptor protein, indicating a potential role in bronchial constriction. These data suggest a possible involvement of the C-terminal splice variant of the NPS receptor in the pathophysiology of asthma, but the report did not describe a functional role for the receptor or its isoforms due to the lack of a pharmacologically useable agonist (Laitinen et al., 2004). Due to

technical constraints, the study also did not distinguish between the Asn^{107} or Ile^{107} isoforms.

In this study we report the pharmacological characteristics of all three human NPS receptor variants and compare them to the murine NPS receptor. The primary structure of NPSR Asn^{107} is identical to isoform A of GPRA. The receptor variant containing isoleucine at position 107 will be referred to as NPSR Ile^{107} and the splice variant containing an alternative C-terminal exon is termed "NPSR C-alt" throughout this manuscript. In this study we demonstrate that a gain-of-function mutation in human NPSR Ile^{107} could have physiological significance in tissues or body functions that involve NPS signaling.

METHODS

Cloning and functional expression of NPSR isoforms – Human NPSR Asn^{107} cDNA was cloned as described before (Xu et al., 2004). The Ile^{107} isoform of NPSR was generated by PCR using synthetic oligonucleotides and the Quik Change Site-Directed Mutagenesis kit from Stratagene. The C-terminal splice variant of NPSR (NPSR C-alt) was generated by recombinant PCR. First, the alternatively spliced exon was cloned by PCR from human genomic DNA using primers NPSRB5 (5'-ATCTCTTTCCCCTGCAGGGTCATCCGTCTCC) and NPSRB3-Xba*I* (5'-TTTCTAGAGAGCTGTCACCTTGGAA, Xba*I* site underlined). Recombinant PCR was

carried out with the cloned exon and human NPSR Asn^{107} cDNA as templates using primers NPSRA5-Xho*I* (5'-ATACTCGAGCCATGCCAGCCAACTTCACAGAGGGCA, Xho*I* site underlined) and NPSRB3-Xba*I*. The products were digested, gel-purified and cloned into pcDNA3.1 hygro (Invitrogen). Mouse NPSR was cloned by nested PCR from mouse total brain cDNA (Clontech). First round primers were 5'-GCTGCAGGTGCAGAGACAGTGAG and 5'-GAGAGCTGACTAAGTTCAGCC. PCR products were further amplified using primers 5'-TTGGATCCCTGCCTGAGCCATGCCA (BamH*I* site underlined) and 5'-TTTCTAGATCAGGGTTTAGATGAATTC (Xba*I* site underlined). The products were digested with the respective restriction enzymes and cloned into pcDNA 3.1 hygro. Transfection of CHO and HEK 293 cells was carried out using lipofectamine (Life Technologies) as described before (Xu et al., 2004). Selection of stable clones was achieved by culturing transfected cells in medium containing 400 mg/l hygromycin (Omega Scientific, Tarzana, CA). For transient expression, transfected cells were cultured for 72 hours without antibiotic selection.

Detection of endogenous NPSR expression in cell lines – Total RNA from a number of human cell lines (HEK293, U373 MG, 1321N, Caco-2, LoVo, DLD-1, Colo205, HCT116, HT-29, SW480, SW1116) was extracted and converted into single-strand cDNA using reverse transcriptase (New England Biolabs) and oligo dT primers. Quantitative real-time PCR was carried out as described using primers specific for human NPSR (Xu et al., 2004).

Measurement of intracellular Ca^{2+} mobilization – Changes of agonist-induced intracellular Ca^{2+} were measured using the FLIPR technology as described before (Xu et al., 2004; Reinscheid et al., 2003). NPS and truncated NPS peptides were a gift from Phoenix Pharmaceuticals (Belmont, CA). Dose-response curves were calculated using GraphPad Prism (Graph Pad, San Diego, CA). Mean EC_{50} values of populations of stable clones expressing individual NPSR variants were compared using unpaired t-test and $p < 0.05$ was considered significant.

Measurement of cAMP accumulation – cAMP was measured as described before (Reinscheid et al., 1996). Briefly, stably transfected cells were seeded into 24-well plates and cultured for 24 hours. Culture medium was aspirated and exchanged for 200 µl Opti-MEM (Life Technologies) containing 100 µM 3-isobutyl-1-methylxanthine and agonists at various concentrations. After incubation for 15 min at 37ºC cells were lysed by adding ethanol to a final concentration of 66%. Aliquots of the lysate were lyophilized and cAMP content was measured in a radioimmunoassay (either Flashplate, NEN Perkin Elmer, or SPA Biotrak, Amersham). Dose response curves were calculated using GraphPad Prism.

CRE-Luciferase reporter gene assays – HEK 293 cells were stably transfected with a reporter gene containing 6 copies of a cAMP response element (CRE; sequence CCAAT) in front of a luciferase reporter gene (Promega) cloned into pcDNA3.1 neo (Himmler et al., 1993). One stable clone showing robust induction of reporter gene expression after forskolin challenge was chosen for further experiments. The different NPSR isoform

cDNAs (cloned into pcDNA3.1 hygro) were transfected into these cells using lipofectamine and stable clones were selected. The same cells and procedures were also used for transient transfection. For induction of reporter gene expression cells were plated in 96-well plates and incubated with agonist for 5 hours in serum-free medium, followed by aspiration of the medium and cell lysis with 25 mM Tris-phosphate, pH 7.8, 2 mM dithiothreitol, 2 mM 1,2-diaminocyclohexane-N,N,N',N',-tetraacetic acid, 10% glycerol, 1 % Triton X-100. After one freeze-thaw cycle aliquots of supernatant were transferred to white clear-bottom 96-well plates (Greiner) and luciferase content was quantified by bioluminescence (Luc-Screen, Applied Biosystems). Plates were counted in a scintillation counter using bioluminescence settings (MicroBeta, Wallac-Perkin Elmer).

Cell proliferation assays – Cells were seeded in 24-well plates and grown overnight to 60-70% confluency. Following 24 h serum-starvation, 2 μCi of methyl-[^{3}H] thymidine was added together with increasing concentrations of NPS. 500 nM PGE_2 served as a positive control. After 3 h incubation cells were washed 3 times with PBS and then lysed with 0.5 N NaOH. The lysate was neutralized with 0.5 N HCl and aliquots were counted in a liquid scintillation counter for incorporated radioactivity.

MAP kinase phosphorylation – Agonist-induced phosphorylation of p42/p44 mitogen-activated protein kinase (MAPK) was determined as described (Saito et al., 2001). Briefly, cells were cultured in 24-well plates in serum-free cell culture medium for 24 h. After stimulation for 5 min at 37ºC with increasing concentrations of NPS, cells were washed with phosphate-buffered saline and lysed with 10 mM Tris-HCl, pH 7.5, 150 mM

NaCl, 5 mM EDTA, 0.1% SDS, 1.5% Nonidet P-40, 0.5% sodium deoxycholate, 1 mM sodium orthovanadate, 1 mM sodium fluoride, 0.5 mM phenylmethylsulfonyl fluoride, 1 μg/ml aprotinin, 0.5 μg/ml leupeptin, 0.7 μg/ml pepstatin, 100 μg/ml bacitracin. Lysates were centrifuged and aliquots of supernatant electrophoresed on 4-10% SDS-polyacrylamide gels. Phosphorylated p42/p44 MAPK was assayed by Western Blot. After transfer to Hybond C membranes (Amersham), blots were incubated with anti-phospho p42/p44 MAPK antibody (Cell Signaling Technologies; dilution 1:1500) in Tris-buffered saline, 1% nonfat dried milk, 0.2% Tween 20 at 4°C overnight. Horseradish peroxidase-conjugated goat anti-rabbit IgG (Jackson Immuno Research Lab; dilution 1:2000) was used as a secondary antibody. Immunoblots were developed using an Enhanced Chemiluminescence detection kit (Amersham) and films were scanned by densitometry (UN-SCAN-IT; Silk Scientific Inc., Orem, UT) for quantitative analysis.

Radioligand binding – Saturation binding experiments in intact cells were carried out exactly as described previously (Xu et al., 2004). K_d and B_{max} of [^{125}I] Y^{10}-NPS binding were calculated using GraphPad Prism. [^{125}I] Y^{10}-NPS was a gift from NEN Perkin-Elmer. Non-specific binding was determined in the presence of 1 μM NPS. Competition binding was measured in HEK cells stably expressing human or mouse NPSR isoforms, respectively, with 0.3 nM [^{125}I] Y^{10}-NPS as tracer.

JPET Fast Forward. Published on September 6, 2005 as DOI: 10.1124/jpet.105.093427
This article has not been copyedited and formatted. The final version may differ from this version.

RESULTS

We have previously described that NPS produces an increase in intracellular Ca^{2+} in cells stably expressing NPSR Asn^{107} with an EC_{50} around 5-10 nM (Xu et al., 2004). Cells transiently transfected with either NPSR Asn^{107}, NPSR Ile^{107} or NPSR C-alt cDNAs did not show agonist-induced changes in Ca^{2+} (data not shown). Also, we could not detect significant receptor binding in transiently transfected cells with any of the constructs, indicating that the proteins might be either difficult to express or expressed at low levels. Therefore, we established stable cells lines expressing either NPSR Asn^{107}, NPSR Ile^{107} or NPSR C-alt in HEK 293 cells.

Three individual cells lines expressing similar levels (~5 fmole/ 10^5 cells) of either human NPSR Asn^{107}, NPSR Ile^{107} or NPSR C-alt were chosen for detailed analyses of pharmacological parameters. As shown in Fig. 2A, NPS induced a dose-dependent increase in intracellular free Ca^{2+} in all cell lines. Cells expressing NPSR Asn^{107} displayed an EC_{50} of 12.4 ± 1.24 nM, whereas the clone expressing NPSR Ile^{107} responded to agonist stimulation with an EC_{50} of 1.4 ± 1.17 nM. Cells stably expressing NPSR C-alt displayed an EC_{50} of 21.7 ± 1.4 nM. As shown in Fig. 2B, NPS also induced cAMP accumulation in HEK cells stably expressing NPSR Asn^{107} with an EC_{50} of 31.9 ± 1.17 nM. In HEK cells expressing NPSR Ile^{107}, NPS stimulated cAMP formation at about ten-fold lower agonist concentrations with an EC_{50} of 3.45 ± 1.26 nM. As mentioned before, we could not observe second messenger signaling in transiently transfected cells

measuring either mobilization of Ca^{2+} or formation of cAMP. However, due to the high rate of signal amplification of the luciferase reporter gene assay, it was possible to establish agonist dose-response curves with this assay in transiently transfected cells. As shown in Fig. 2C, NPSR Asn^{107} displayed only a weak induction of luciferase activity with an EC_{50} of 76.6 ± 21.5 nM. In contrast, NPSR Ile^{107} produced a robust increase in reporter gene expression with an EC_{50} of 17.3 ± 1.31 nM. The NPSR variant containing the alternatively spliced C-terminus (NPSR C-alt) displayed an EC_{50} of 146.5 ± 15.1 nM, similar to the NPSR Asn^{107} variant. The maximum of reporter gene expression in HEK cells transiently transfected with NPSR Ile^{107} was about 2 fold higher than in cells expressing NPSR Asn^{107} or NPSR C-alt, suggesting an increase in agonist efficacy. The magnitude of reporter gene induction was about 20-fold lower in transiently transfected cells as compared to stable clones (see below).

In order to investigate whether this increase in agonist potency at NPSR Ile^{107} was a general property of the receptor protein we compared a large number of stable clones expressing either NPSR Asn^{107}, NPSR Ile^{107} or NPSR C-alt by establishing dose-response curves for each construct and calculating mean EC_{50} values for the populations. As shown in Fig. 3, the mean EC_{50} for NPS-induced mobilization of intracellular Ca^{2+} at NPSR Asn^{107} was found to be 13.02 ± 1.18 nM (n = 16 individual stable clones). In contrast, NPSR Ile^{107} displayed a more than ten-fold lower mean EC_{50} of 1.01 ± 0.13 nM (n = 21). In the clones expressing NPSR C-alt the peptide showed a mean EC_{50} of 32.5 ± 1.15 nM (n = 14). These data demonstrate that NPSR Ile^{107} is activated by significantly

JPET Fast Forward. Published on September 6, 2005 as DOI: 10.1124/jpet.105.093427
This article has not been copyedited and formatted. The final version may differ from this version.

lower concentrations of agonist than NPSR Asn^{107} or NPSR C-alt ($F_{2,51}$ = 79.65; p < 0.0001).

Using the same approach as described before, we compared the EC_{50} values of a large number of stable clones established in HEK cells that co-express the CRE-Luciferase reporter gene. As shown in Fig. 3, HEK cells stably expressing both NPSR Asn^{107} and the reporter gene displayed a mean EC_{50} of 45.08 ± 1.19 nM for NPS-induced reporter gene expression (n = 7 individual clones). In contrast, cells co-expressing NPSR Ile^{107} and the reporter gene showed a mean EC_{50} of 0.63 ± 0.43 nM for NPS (n = 21). Cells expressing NPSR C-alt displayed a mean EC_{50} of 28.8 ± 1.42 nM in the reporter gene assay (n = 12). Again, these data indicate that NPSR Ile^{107} is activated at significantly lower agonist concentrations than NPSR Asn^{107} or the alternatively spliced NPS receptor ($F_{2,37}$ = 67.31; p = 0.0001). Taken together, these data indicate that the Ile^{107} mutation produces a gain-of-function in the NPS receptor protein, whereas the alternatively spliced C-terminus does not appear to affect agonist potency.

Many GPCRs have been shown to affect cell growth that might have significance in malignant or other pathological processes. In order to investigate whether NPSR can affect cell proliferation at natural levels of receptor expression, we screened a number of cancer cell lines for endogenous NPSR mRNA expression by RT-PCR. The human colon cancer line Colo205 was found to express NPSR transcripts but did not display agonist-induced second messenger responses (data not shown). However, NPS produced a dose-dependent stimulation of thymidine incorporation in Colo205 cells, indicating that the

JPET Fast Forward. Published on September 6, 2005 as DOI: 10.1124/jpet.105.093427
This article has not been copyedited and formatted. The final version may differ from this version.

peptide can stimulate cell proliferation and mitogenic signals in these cells (Fig. 4A). Doses of 0.1-10 nM NPS produced maximal thymidine incorporation, exceeding the effect of the well-characterized mitogen prostaglandin E2 (PGE_2) on these cells. The human colon cancer cell line DLD-1, which does not express NPSR transcripts, served as a negative control and showed no NPS-dependent thymidine incorporation (data not shown). We next examined potential intracellular mediators of the proliferative response elicited by NPS. The p42/p44 mitogen-activated protein kinase (MAPK) is a well-known integrator of mitogenic signals and many GPCRs have been shown to increase phosphorylation of MAPK upon agonist stimulation. We found that NPS can stimulate MAPK phosphorylation in a dose-dependent manner in HEK cells stably expressing NPSR Asn^{107} or NPSR Ile^{107} isoforms. As observed before, NPS was more potent to induce MAPK phosphorylation in cells expressing NPSR Ile^{107} (EC_{50}: 0.32 ± 0.25 nM) than in cells expressing NPSR Asn^{107} (EC_{50}: 1.23 ± 0.38 nM) (Fig. 4B).

Two individual clones, expressing either NPSR Asn^{107} or NPSR Ile^{107} with EC_{50} values close to the average EC_{50} in mobilizing intracellular Ca^{2+}, were chosen to examine the structure-activity relationships of various NPS fragments. These NPS fragments represent potential processing products that could result from proteolytic cleavage or human NPS 1-20. In addition, we also tested the effect of rat and mouse NPS 1-20 on these cells. As shown in Fig. 5A and B and Table 1, most carboxy-terminally truncated fragments of NPS retained full agonist potency at both NPSR isoforms. Rat and mouse NPS 1-20 appear to be slightly more potent agonists at both NPSR isoforms as compared to the human peptide. Interestingly, NPS 1-12 shows greatly decreased agonist activity at

JPET Fast Forward. Published on September 6, 2005 as DOI: 10.1124/jpet.105.093427
This article has not been copyedited and formatted. The final version may differ from this version.

NPSR Asn^{107} while still behaving as a full, but weakly potent, agonist at NPSR Ile^{107}. Further deletion of the two lysine residues at position 11 and 12 produced NPS 1-10. NPS 1-10 displayed full agonist activity at both NPSR isoforms, albeit with significantly higher potency at NPSR Ile^{107}. Deletion of the three amino-terminal amino acids (NPS 4-20) completely abolished agonist activity. These data indicate that the N-terminus of NPS contains the pharmacophore. The two lysine residues at position 11 and 12 appear to attenuate activation of the receptor when exposed at the C-terminus because further C-terminal deletion to NPS 1-10 restored agonist activity. Because of the peculiar pharmacology of NPS 1-12, this fragment was also tested for possible antagonist activity but failed to block activation of the two human receptor isoforms by NPS 1-20 (data not shown). Overall, the various NPS fragments displayed a 5-10 fold higher potency at NPSR Ile^{107} as compared to NPSR Asn^{107} (Table 1).

Some of the previous observations could be explained by an increased affinity or higher receptor expression of NPSR Ile^{107} versus NPSR Asn^{107}. We therefore determined receptor binding parameters in a number of stable clones for both variants. Surprisingly, both NPSR Asn^{107} and NPSR Ile^{107} bind the radioligand with very similar affinities (K_d range of NPSR Asn^{107} clones: 0.2 - 0.45 nM, n = 4, average K_d: 347.1 ± 44 pM; K_d range of NPSR Ile^{107} clones: 0.17 – 0.5 nM, n = 4, average K_d: 402.5 ± 49 pM). However, stable NPSR Ile^{107} clones tended to express more functional receptor protein per cell than NPSR Asn^{107} clones (average B_{max} of NPSR Ile^{107} clones: 12.5 ± 3.5 fmole/10^5 cells; average B_{max} of NPSR Asn^{107} clones: 3.9 ± 1.5 fmoles/10^5 cells; n = 4 for each receptor variant). Overall, the levels of NPS receptor expression are low compared to other

GPCRs expressed in the same cellular environment. Dose-response relationship experiments for Ca^{2+} mobilization, cAMP formation and MAPK phosphorylation were performed with individual clones that display very similar receptor levels in order to correct for possible confounds caused by varying numbers of functional receptors (Figs. 2A, 2B, and 4B). Taken together, our data indicate that the increased potency of NPS at NPSR Ile^{107} is not caused by a change in receptor affinity but might reflect an increased intrinsic efficacy of the receptor protein to couple to G proteins and thus to the various second messenger pathways, as described above.

We also investigated the pharmacological profile of the mouse NPS receptor since much *in vivo* studies on the physiological functions of NPS have been performed in this species (Xu et al., 2004) and increased expression of NPSR has been reported in a murine model of allergic airway inflammation (Laitinen et al., 2004). The mouse NPSR carries an Ile residue at amino acid position 107 and currently available genetic data do not indicate polymorphic variants at this site in the mouse genome. As shown in Fig. 5C and Table 1, HEK cells stably expressing mouse NPSR responded to stimulation with various NPS peptides by increasing intracellular free Ca^{2+}. The EC_{50} values and rank order of potency of the various NPS peptides for mobilizing Ca^{2+} were found to lie in between those obtained with cells expressing human NPSR Asn^{107} or NPSR Ile^{107}, respectively Mouse and rat NPS appear to be slightly more potent at mouse NPSR. In contrast to the human NPSR isoforms, the rank order of potency for NPS 1-12 and NPS 1-10 was reversed, indicating that the two carboxyterminal lysine residues in NPS 1-12 might interact differently with mouse NPSR than with the human receptors. When analyzing a

JPET Fast Forward. Published on September 6, 2005 as DOI: 10.1124/jpet.105.093427
This article has not been copyedited and formatted. The final version may differ from this version.

population of individual HEK clones stably expressing mouse NPSR we obtained a mean EC_{50} value of 4.58 ± 1.28 nM (n = 15 individual clones; Fig. 3). Statistical analysis indicated that the mean EC_{50} of mouse NPSR was significantly different from both human NPSR Asn^{107} ($p < 0.05$) and human NPSR Ile^{107} ($p < 0.05$). Radioligand binding experiments showed that mouse NPSR binds NPS with approximately the same affinity as compared to the human NPS receptor variants (Fig. 6). Note that the IC_{50} values for halfmaximal displacement of the radioligand in stable HEK cells are about tenfold higher than in CHO cells (IC_{50} [CHO] = 0.4 nM; IC_{50} [HEK] = 4 nM) that we reported previously (Xu et al., 2004).

DISCUSSION

In the present study we have investigated the pharmacological properties and signal transduction pathways of three natural variants of the human NPS receptor and the orthologous mouse protein. We also sought to determine whether the coding polymorphism or alternative splicing of human NPSR would affect the receptor pharmacology in a way that might have functional significance for the pathophysiology of asthma, since the human NPS receptor was recently identified as an asthma susceptibility gene (Laitinen et al., 2004).

Our data provide evidence for an increased agonist potency at human NPSR Ile^{107}. Surprisingly, the Asn^{107}Ile point mutation does not affect ligand binding affinity, even

JPET Fast Forward. Published on September 6, 2005 as DOI: 10.1124/jpet.105.093427
This article has not been copyedited and formatted. The final version may differ from this version.

though this amino acid is expected to be close to the ligand binding pocket of the receptor protein (Fig. 1). The endogenous agonist NPS displays about a ten-fold higher potency at NPSR Ile^{107} as compared to NPSR Asn^{107} in mobilizing intracelluar Ca^{2+}, stimulating cAMP formation or inducing MAPK phosphorylation. The Ile^{107} mutation does not produce increased constitutive activity, as judged from the cAMP accumulation and reporter gene assays. A plausible explanation for our observations could be that the Asn^{107}Ile polymorphism is producing a conformational change of the receptor protein that facilitates agonist-induced G protein interaction and thus increases agonist potency in NPSR Ile^{107}. However, the Ile residue at position 107 is not solely sufficient to convey increased agonist potency since mouse NPSR, which also carries an Ile residue at this position, displays intermediate agonist potencies when compared to human NPSR Asn^{107} and NPSR Ile^{107}, respectively. We also observed a trend to higher levels of receptor protein expression in stable clones expressing human NPSR Ile^{107}. It is currently not known if NPSR Ile^{107} expression is also facilitated *in vivo* or if our observation is due to the over-expression system used in our studies. Together, our data indicate that the Asn^{107}Ile polymorphism in human NPSR produces a gain-of-function that could have significant functional consequences in physiological processes that involve NPS signaling.

The C-terminal splice variant of NPSR (NPSR C-alt, GPRA isoform B) was described to be significantly over-expressed in airway smooth muscle cells from asthmatic patients as compared to healthy controls when studied by immunohistochemical staining (Laitinen et al., 2004). Our data provide no evidence for

an altered second messenger response elicited by NPSR C-alt as compared to NPSR Asn^{107}. Both receptor variants contain an Asn residue at position 107. It remains to be determined whether the alternative C-terminal tail of the receptor protein can affect other signaling pathways or receptor desensitization and thus have functional significance. Interestingly, the alternative exon giving rise to NPSR C-alt in human is absent from the mouse and rat genome.

Our data show that NPSR can couple to intracellular Ca^{2+} as well as cAMP pathways, indicating interaction with both G_q and G_s types of G proteins. The pharmacophore of NPS is contained within the N-terminal part of the peptide and we describe NPS 1-10 as a minimally active structure. All NPS fragments used in our studies could be produced by proteolytic processing involving trypsin-like cleavage at basic amino acid residues. Some of these fragments retain potent agonist activity. Therefore, it will be important to determine the enzymatic steps involved in the inactivation of this neuropeptide *in vivo*. Apparently the NPSR protein cannot be studied easily in transient transfection systems which made the pharmacological analysis of the receptor variants more tedious. One common problem of using stable clones for second messenger assays is caused by the fact that each clone displays an individual pharmacology and comparison of too few stable clones can lead to inaccurate assumptions about general pharmacological properties. Therefore, we chose to analyze a large population of stable clones and determined mean EC_{50} values, followed by statistical analysis. This procedure allowed us to detect significant differences in agonist-induced second messenger coupling between the NPSR Asn^{107}, NPSR Ile^{107} and NPSR C-alt isoforms, respectively.

JPET Fast Forward. Published on September 6, 2005 as DOI: 10.1124/jpet.105.093427
This article has not been copyedited and formatted. The final version may differ from this version.

At present, the functional involvement of NPSR in airway smooth muscle contraction still remains to be verified. According to the report by Laitinen et al., the receptor protein appears to be expressed in airway smooth muscle cells that might contribute to bronchial constriction (Laitinen et al., 2004). Our data indicate that activation of NPSR produces an increase in intracellular free Ca^{2+} and that the NPSR Ile^{107} variant, if expressed in airway smooth muscle cells, could thus transmit an enhanced contractile response requiring lower agonist concentrations. Since increased bronchial constriction is one of the physiological hallmarks of asthma (Bousquet et al., 2000), the gain-of-function mutation in NPSR Ile^{107} could therefore be associated with this phenotype. Also, our studies provide evidence for a proliferative effect of NPS using a cellular model of endogenous NPSR expression and demonstrating enhanced phosphorylation of MAPK. Tissue remodeling in asthmatic airways involves proliferation of smooth muscle cells and thickening of basal membranes (Bousquet et al., 2000). It remains to be determined whether these pathological changes are influenced by NPS receptors endogenously expressed in airway smooth muscle cells. Therefore, further investigations into the functional role of NPSR in airway tissue will be necessary to determine whether the gain-of-function polymorphism in NPSR Ile^{107} that we describe in this paper might be involved in any of the pathological events underlying asthma. Ultimately the development of NPS antagonists will be a critical step to fully understand the physiological functions of NPS signaling.

Naturally occurring polymorphisms that affect receptor function have been identified in numerous GPCRs. Not surprisingly, most of these mutations lead to inactive receptor proteins. The few examples of gain-of-function mutations can be divided into two classes based on their pharmacological phenotype: One group of mutations produces constitutively active receptors that promote second messenger signaling in the absence of endogenous agonist. This type of activating mutations has been found in the glycoprotein-hormone receptor subfamily (LH and TSH receptor), parathyroid and parathyroid-related peptide receptor, as well as in rhodopsin (Spiegel and Weinstein, 2004). The other type of activating polymorphisms increases ligand affinity or agonist efficacy in a way similar to the NPSR Ile^{107} variant. Such mutations have been found in the Ca^{2+}-sensing receptor and result in hypocalcemia and hypercalciuria (Pollak et al., 1994).

Genetic variations in several GPCRs have also been associated with asthma susceptibility or effectiveness of asthma pharmacotherapy. A coding polymorphism in the cysteinyl-leukotriene receptor type 2 (CysLT2) was found to reduce the receptor's affinity to one of its major endogenous ligands, leukotriene D_4 (LTD_4). Since LTD_4 is an important mediator of inflammatory responses in asthma this polymorphism in CysLT2 provides an asthma-protective effect (Pillai et al., 2004). Similarly, particular haplotypes in the promotor region of the prostanoid DP receptor (PTGDR) were found underrepresented in asthmatic patients. These polymorphisms lead to a reduced transcription of PTGDR mRNA and thus lower levels of receptor protein. Prostaglandin D2 (the endogenous ligand of PTGDR) is an important mediator of asthma and PTGDR

was found to be required for the development of airway sensitization in a mouse model of asthma. This might explain why reduced levels of PTGDR expression lead to an overall asthma-protective effect (Oguma et al., 2004). Coding polymorphisms in the β_2-adrenoreceptor that influence receptor downregulation in response to adrenergic agonists were found to be associated with the therapeutic benefit of β_2-agonists to treat symptoms of asthma (Israel et al., 2004). Although β_2-adrenoreceptors are not causally involved in the pathophysiology of asthma, they are important therapeutic targets for acute and intermittent treatment of asthma symptoms. These examples illustrate the important contribution of specific GPCR genotypes for asthma susceptibility or therapy.

The observation of enhanced NPS-induced second messenger responses at NPSR Ile^{107} could also have important consequences for brain function since the predominant sites of NPSR expression are found in the central nervous system (Xu et al., 2004). It might be possible that the Ile^{107} isoform of NPSR is associated with changes in behavior or neuronal processing. In summary, we provide evidence that a naturally occurring polymorphism in the NPS receptor is producing a gain-of-function, resulting in enhanced second messenger signaling. Future research will have to demonstrate whether this polymorphism has functional significance in asthma or other physiological processes involving NPS signaling.

ACKNOWLEDGEMENTS

The authors would like to thank Phoenix Pharmaceuticals and NEN Perkin Elmer for generous supply of research materials.

REFERENCES

Bousquet J, Jeffrey PK, Busse WW, Johnson M and Vignola A (2000) Asthma: from bronchoconstriction to airways inflammation and remodeling. *Am J Respir Crit Care Med* 161:1720-1745.

Himmler A, Stratowa C and Czernilofsky AP (1993) Functional testing of human dopamine D1 and D5 receptors expressed in stable cAMP-responsive luciferase reporter cell lines. *J Recept Res* 13:79-94.

Hofmann K and Stoffel W (1993) TMbase - A database of membrane spanning proteins segments. *Biol Chem Hoppe-Seyler* 374:166-173.

Israel E, Chinchilli VM, Ford JG, Boushey HA, Cherniack R, Craig TJ, Deykin A, Fagan JK, Fahy JV, Fish J, Kraft M, Kunselman SJ, Lazarus SC, Lemanske RF Jr, Liggett SB, Martin RJ, Mitra N, Peters SP, Silverman E, Sorkness CA, Szefler SJ, Wechsler ME, Weiss ST, Drazen JM; National Heart, Lung, and Blood Institute's Asthma Clinical Research Network. (2004) Use of regularly scheduled albuterol treatment in asthma: genotype-stratified, randomised, placebo-controlled cross-over trial. *Lancet* 364:1505-1512.

Laitinen T, Polvi A, Rydman P, Vendelin J, Pulkkinen V, Salmikangas P, Makela S, Rehn M, Pirskanen A, Rautanen A, Zucchelli M, Gullsten H, Leino M, Alenius H, Petays

T, Haahtela T, Laitinen A, Laprise C, Hudson TJ, Laitinen LA and Kere J (2004) Characterization of a common susceptibility locus for asthma-related traits. *Science* 304:300-304.

Oguma T, Palmer LJ, Birben E, Sonna LA, Asano K and Lilly CM (2004) Role of prostanoid DP receptor variants in susceptibility to asthma. *N Engl J Med* 351:1752-1763.

Pillai SG, Cousens DJ, Barnes AA, Buckley PT, Chiano MN, Hosking LK, Cameron LA, Fling ME, Foley JJ, Green A, Sarau HM, Schmidt DB, Sprankle CS, Blumenthal MN, Vestbo J, Kennedy-Wilson K, Wixted WE, Wagner MJ, Anderson WH, Ignar DM; Investigators of the GAIN Network. (2004) A coding polymorphism in the CYSLT2 receptor with reduced affinity to LTD4 is associated with asthma. *Pharmacogenetics* 14:627-633.

Pollak MR, Brown EM, Estep HL, McLaine PN, Kifor O, Park J, Hebert SC, Seidman CE and Seidman JG (1994) Autosomal dominant hypocalcaemia caused by a Ca(2+)-sensing receptor gene mutation. *Nat Genet* 8:303-307.

Reinscheid RK, Ardati A, Monsma FJ and Civelli O (1996) Structure-activity relationship studies on the novel neuropeptide orphanin FQ. *J Biol Chem* 271:14163-14168.

Reinscheid RK, Kim J, Zeng J and Civelli, O. (2003) High-throughput real-time assay for monitoring Gs-coupled receptor activation in intact cells. *Eur J Pharmacol* 478:27-34.

Saito Y, Wang Z, Hagino-Yamagishi K, Civelli O, Kawashima S and Maruyama K. (2001) Endogenous melanin-concentrating hormone receptor SLC-1 in human melanoma SK-MEL-37 cells. *Biochem Biophys Res Commun* 289:44-50.

Spiegel AM and Weinstein LS (2004) Inherited diseases involving G proteins and G protein-coupled receptors. *Annu Rev Med* 55:27-39.

Xu Y-L, Reinscheid RK, Huitron-Resendiz S, Clark SD, Wang Z, Lin SH, Brucher FA, Zeng J, Ly NK, Henriksen SJ, de Lecea L and Civelli O (2004) Neuropeptide S: A neuropeptide promoting arousal and anxiolytic-like effects. *Neuron* 43:487–497.

FOOTNOTES

This study was supported in part by grants from NIMH and NARSAD to R.K.R. and grants from NIMH and the Stanley Medical Research Institute to O.C.

Reprint requests should be addressed to: Rainer K. Reinscheid, Department of Pharmacology, University of California Irvine, 360 Med Surge II, Irvine, CA 92697-4625, email: rreinsch@uci.edu

JPET Fast Forward. Published on September 6, 2005 as DOI: 10.1124/jpet.105.093427
This article has not been copyedited and formatted. The final version may differ from this version.

FIGURE LEGENDS

Fig. 1: Schematic diagram ("snake plot") of the human NPS receptor protein showing the presumed location of the Asn^{107}Ile polymorphism and the sequence of the alternatively spliced carboxy-terminal tail in NPSR C-alt. Putative transmembrane domains are boxed and were predicted with TMPred (www.ch.embnet.org/software/TMPRED_form.html; Hofmann and Stoffel, 1993).

Fig. 2: Pharmacological activity of NPS at NPSR Asn^{107}, NPSR Ile^{107} and NPS C-alt. *A*, dose-response curves of NPS to elicit mobilization of intracellular Ca^{2+} in HEK 293 cells stably expressing either NPSR Asn^{107}, NPSR Ile^{107} or NPS C-alt. NPS displays greater agonist potency at NPSR Ile^{107}. Incubations were performed in triplicate and repeated three times. Data are shown as means ± SEM. *B*, dose-response curve of NPS to stimulate cAMP formation in two individual HEK 293 clones expressing either NPSR Asn^{107} or NPSR Ile^{107}. NPS displays greater agonist potency at NPSR Ile^{107}. Incubations were performed in triplicate and repeated three times. Data are shown as means ± SEM. *C*, dose-response curves of NPS stimulating CRE-mediated luciferase reporter gene expression. HEK 293 cells were transiently transfected with plasmids containing either NPSR Asn^{107}, NPSR Ile^{107} or NPSR C-alt cDNA constructs. Bioluminescence was determined from triplicate incubations repeated at least twice and data are presented as means ± SEM.

JPET Fast Forward. Published on September 6, 2005 as DOI: 10.1124/jpet.105.093427
This article has not been copyedited and formatted. The final version may differ from this version.

Fig. 3: Scatter-plot of logarithmic EC_{50} values of individual HEK 293 clones expressing human NPSR Asn^{107} (Asn^{107}), NPSR Ile^{107} (Ile^{107}) or NPSR C-alt (C-alt) and mouse NPSR (mNPSR). Dose-response curves for each individual clone were established measuring either mobilization of intracellular Ca^{2+} (left) or induction of luciferase reporter gene transcription (right). Horizontal bars indicate mean EC_{50} values.

Fig. 4: NPS effect on cell proliferation and MAPK phosphorylation. *A*, NPS-induced stimulation of [^{3}H]-thymidine incorporation in Colo205 human colon cancer cells. NPS produces a dose-dependent stimulation of cell proliferation. 500 nM PGE_2 was used as a positive control. All incubations were performed in triplicates and experiments were repeated twice. Data are shown as means ± SEM. ** $p < 0.01$ vs. buffer control. *B*, stimulation of MAPK phosphorylation by increasing concentrations of NPS. Values were normalized to levels of phospho-MAPK produced by incubation with 1 μM NPS (= 100%). Phospho-MAPK was quantified by densitometric scanning of Western Blots as described under "Materials and Methods". Assays were performed in duplicate and repeated twice. Data are shown as means ± SEM.

Fig. 5: Structure-activity relationships of NPS peptides and truncated NPS fragments at human or mouse NPSR variants. Ca^{2+} mobilization elicited by human (h), mouse (m) or rat (r) NPS and various NPS fragments was determined in individual HEK 293 clones expressing either NPSR Asn^{107} (*A*), NPSR Ile^{107} (*B*), or mouse NPSR (*C*). Dose-response

JPET Fast Forward. Published on September 6, 2005 as DOI: 10.1124/jpet.105.093427
This article has not been copyedited and formatted. The final version may differ from this version.

curves were calculated from triplicate incubations and all assays were repeated at least twice. See Table 1 for comparison of EC_{50} values and peptide sequences. Data from triplicate experiments are shown as means ± SEM.

Fig. 6: Radioligand binding. Displacement of 0.3 nM [^{125}I] Y^{10}-NPS by increasing concentrations of unlabeled human NPS in HEK cells stably expressing either human NPSR Asn^{107}, NPSR Ile^{107} or mouse NPSR. Data from triplicate experiments were normalized to correct for different levels of receptor expression and are shown as means ± SEM.

Table 1: EC_{50} values (nM, ± SEM) of NPS peptides and NPS fragments at human and mouse NPSR isoforms

Peptide	Sequence	hNPSR Asn^{107}	hNPSR Ile^{107}	mNPSR
hNPS 1-20	SFRNGVGTGMKKTSFQRAKS	8.43 ± 1.47	1.78 ± 1.31	4.66 ± 1.13
hNPS 1-18	SFRNGVGTGMKKTSFQRA	10.9 ± 1.2	2.59 ± 1.45	7.85 ± 1.2
rNPS 1-20	SFRNGVGSGVKKTSFRRAKQ	3.1 ± 1.34	0.86 ± 0.13	1.11 ± 0.8
mNPS 1-20	SFRNGVGSGAKKTSFRRAKQ	2.8 ± 1.37	0.77 ± 0.14	0.99 ± 0.24
hNPS 1-12	SFRNGVGTGMKK	> 10.000	2520 ± 118	32.5 ± 5.9
rNPS 1-10	SFRNGVGSGV	2090 ± 238	18.8 ± 13.6	98.4 ± 7.8
hNPS 4-20	NGVGTGMKKTSFQRAKS	inactive	inactive	inactive

All peptides were tested for mobilization of intracellular Ca^{2+} in independent stable clones expressing the respective NPSR isoform. EC_{50} values were calculated from triplicate incubations. Data from typical experiments are shown. The human NPS 1-10 peptide was insoluble and could not be tested; h, human; m, mouse; r, rat.

JPET Fast Forward. Published on September 6, 2005 as DOI: 10.1124/jpet.105.093427
This article has not been copyedited and formatted. The final version may differ from this version.

Fig. 1

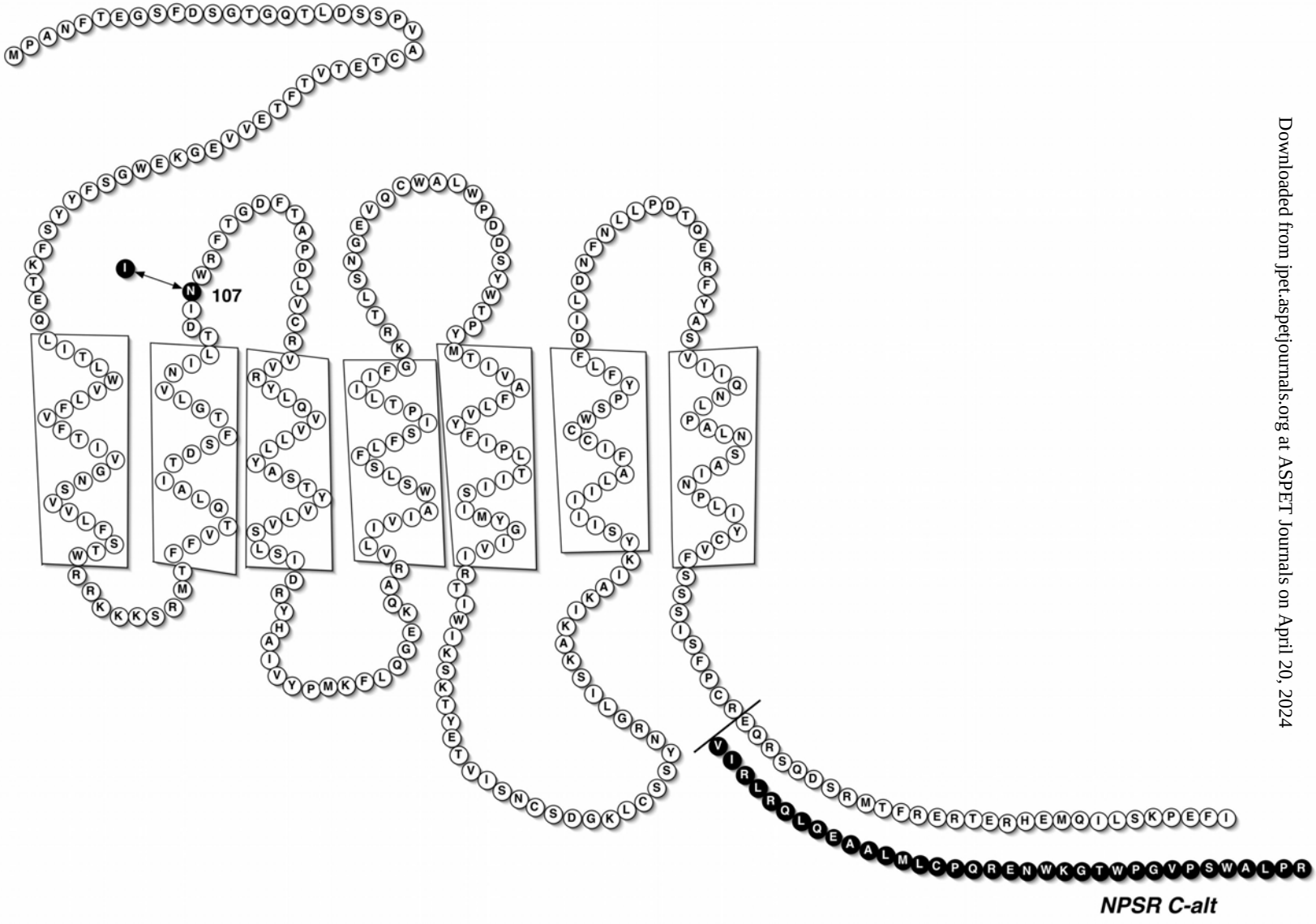

JPET Fast Forward. Published on September 6, 2005 as DOI: 10.1124/jpet.105.093427
This article has not been copyedited and formatted. The final version may differ from this version.

Fig. 2

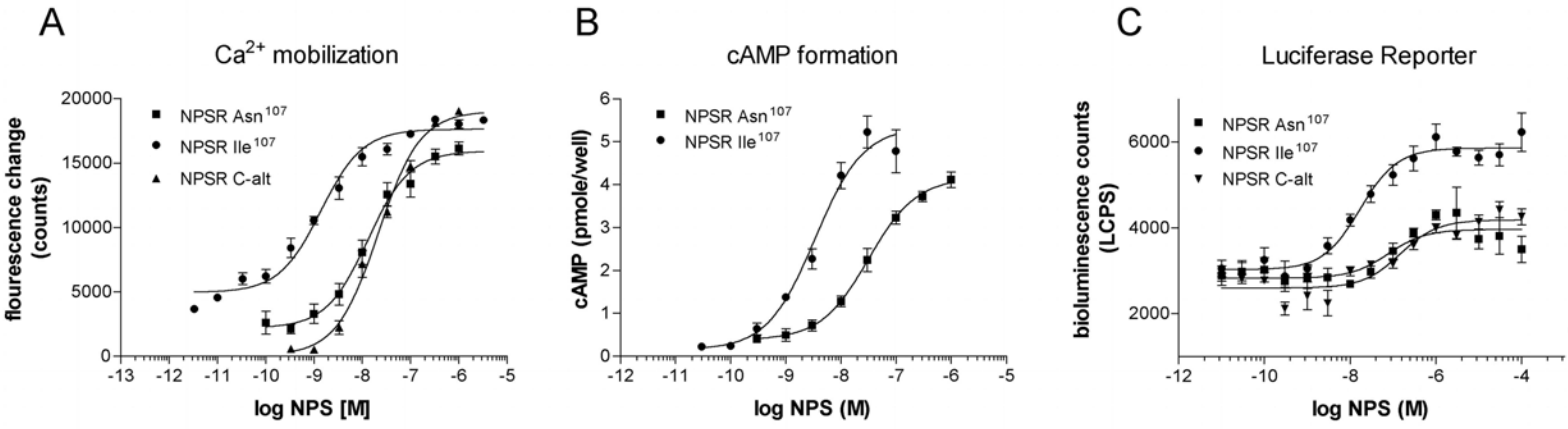

JPET Fast Forward. Published on September 6, 2005 as DOI: 10.1124/jpet.105.093427
This article has not been copyedited and formatted. The final version may differ from this version.

Fig. 3

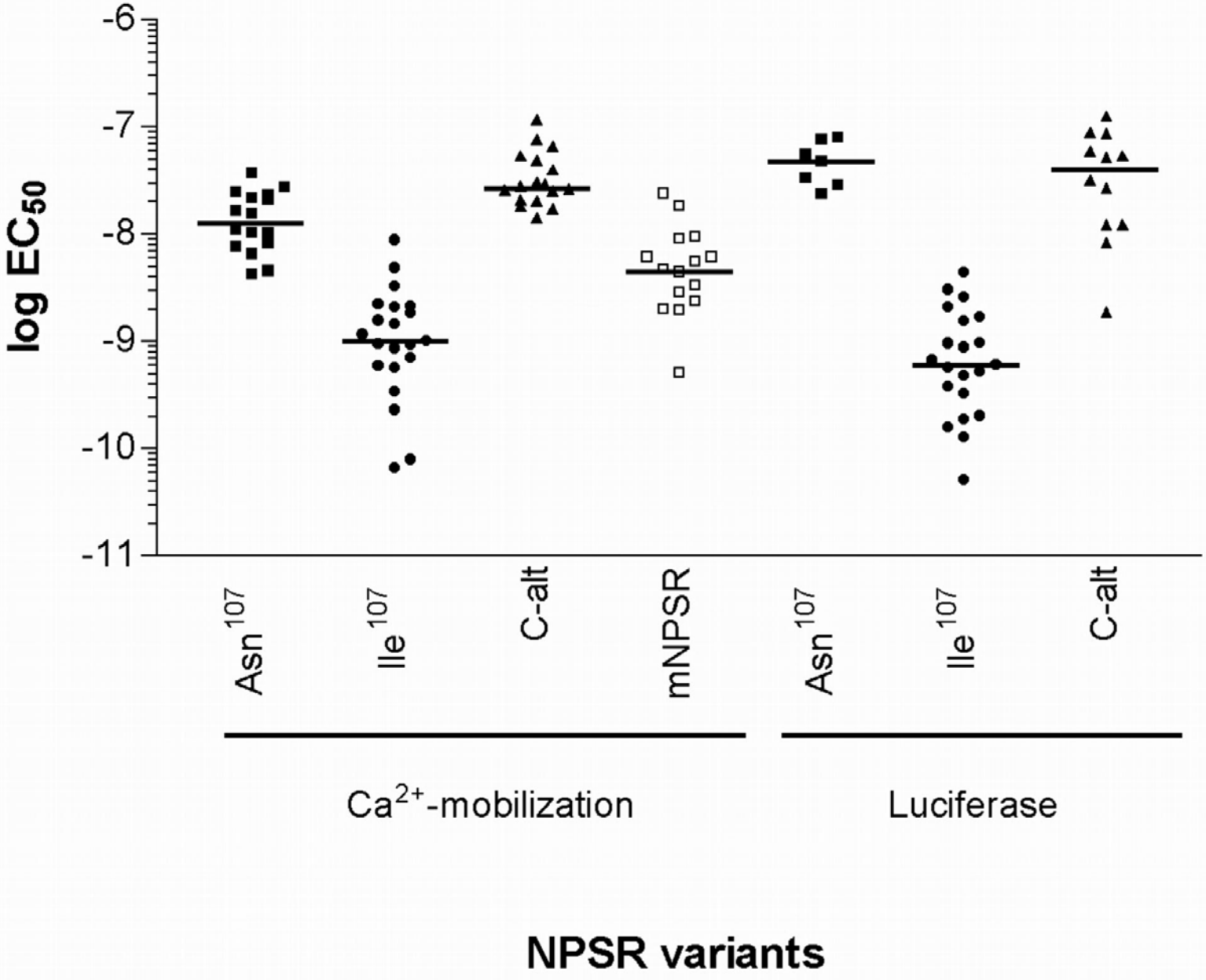

JPET Fast Forward. Published on September 6, 2005 as DOI: 10.1124/jpet.105.093427
This article has not been copyedited and formatted. The final version may differ from this version.

Fig. 4

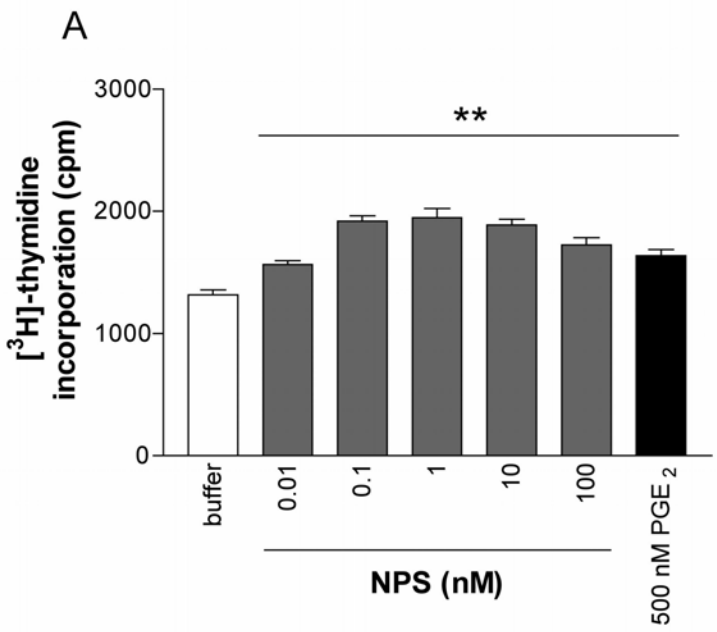

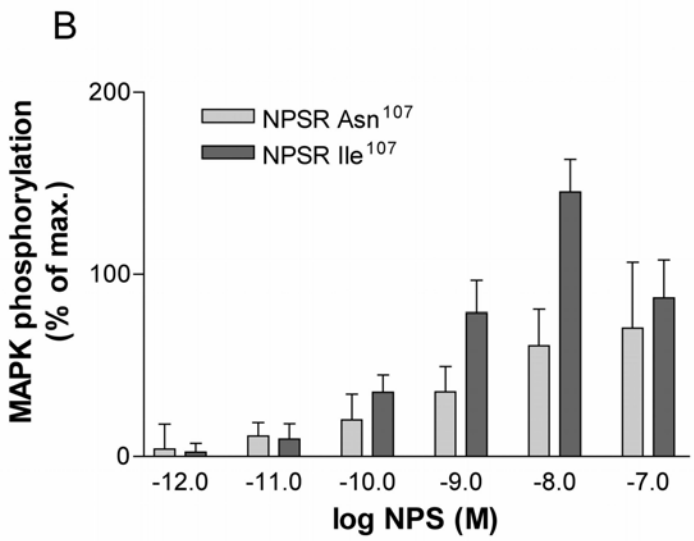

JPET Fast Forward. Published on September 6, 2005 as DOI: 10.1124/jpet.105.093427
This article has not been copyedited and formatted. The final version may differ from this version.

Fig. 5

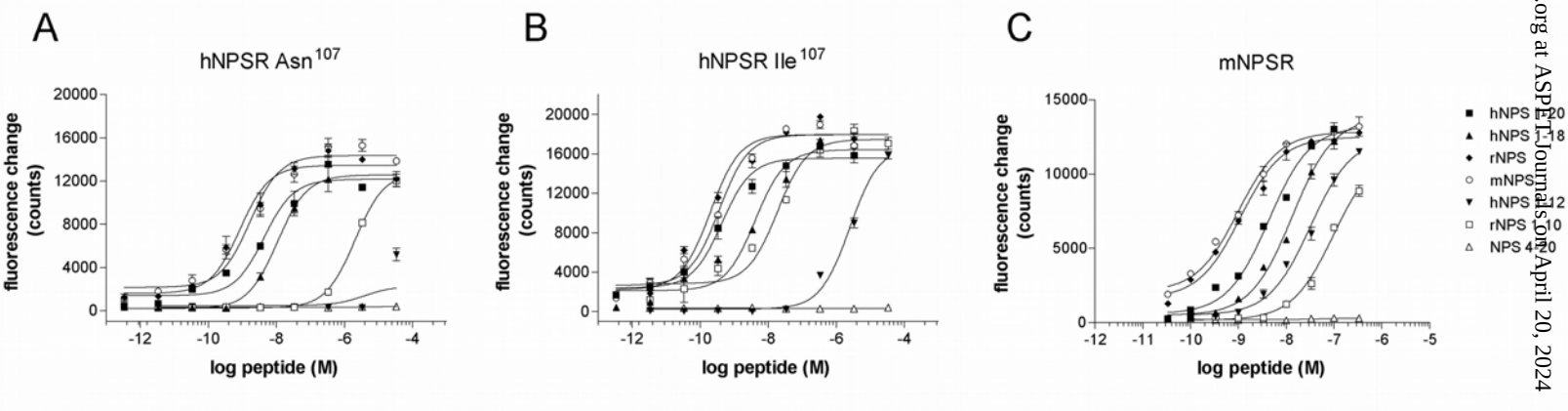

JPET Fast Forward. Published on September 6, 2005 as DOI: 10.1124/jpet.105.093427
This article has not been copyedited and formatted. The final version may differ from this version.

Fig. 6